

# Different technical possibilities of post-therapeutic tandem $^{90}\text{Y}/^{177}\text{Lu}$ -DOTATATE imaging

Jolanta Kunikowska<sup>1</sup>, Adam Bajera<sup>1</sup>, Magdalena Sawicka<sup>1</sup>, Piotr Czwarnowski<sup>1</sup>, Bożena Pawłowicz<sup>1</sup>, Dariusz Aksamit<sup>1</sup>, Dariusz Pawlak<sup>2</sup>, Leszek Królicki<sup>1</sup>

<sup>1</sup>Nuclear Medicine Department, Medical University of Warsaw, Poland

<sup>2</sup>National Centre for Nuclear Research, Radioisotope Centre POLATOM, Otwock-Świerk, Poland

[Received 3 VI 2013; Accepted 10 VI 2013]

## Abstract

**BACKGROUND:** Neuroendocrine tumors (NETs) are a heterogeneous group of neoplasms derived from endocrine stem cells. These tumors are characterized by overexpression of somatostatin receptors (SSTR), which is utilized for imaging using SSTR analogs. Peptide receptor radionuclide therapy (PRRT) somatostatin analogs labeled with  $^{90}\text{Y}$  and  $^{177}\text{Lu}$  in neuroendocrine tumors (NETs) results in symptomatic improvement, prolonged survival, and enhanced quality of life. The post-therapeutic imaging leads to possibility of biodistribution of therapy.

The aim of our study was to describe different possibilities of post-therapeutic imaging in patients underwent tandem therapy  $^{90}\text{Y}/^{177}\text{Lu}$ -DOTATATE with preliminary results of  $^{90}\text{Y}$  PET imaging.

**MATERIAL AND METHODS:** Thirty patients (11 men, 19 women; the mean age  $55 \pm 10.9$  y) with histological confirmation of metastatic neuroendocrine tumors (G1 and G2) were treated with tandem therapy  $^{90}\text{Y}/^{177}\text{Lu}$ -DOTATATE. WHBA scan and SPECT acquisition of the abdomen were performed 24 hours post therapy injection, on the dual-head Varicam camera (ELSCINT) using  $^{177}\text{Lu}$  photopeak and  $^{90}\text{Y}$  *bremsstrahlung*. PET imaging of  $^{90}\text{Y}$  component was done on Siemens Biograph Truepoint PET/CT (window  $511 \text{ keV} \pm 15\%$ )

4 hours after  $^{90}\text{Y}/^{177}\text{Lu}$ -DOTATATE. Additionally phantom studies were performed to analyze the spatial resolution of different protocols.

**RESULTS:** Out of all the patients, median OS was 49.8 months and median EFS time 24.3 months. Spatial resolution achieved for  $^{90}\text{Y}$ ,  $^{177}\text{Lu}$  and PET imaging of  $^{90}\text{Y}$  component measured using the phantom of the torso filled up with water was 20 mm, 8mm and 4–5 mm FWHM, respectively. Spatial resolution in human body in our study was about 30 mm for  $^{90}\text{Y}$ , 15 mm for  $^{177}\text{Lu}$  and 25–30 mm for PET imaging of  $^{90}\text{Y}$  component.

**CONCLUSIONS:** The theoretically best spatial resolution offers PET scanner, however it is important to keep in mind that  $^{90}\text{Y}$ -imaging PET is not used for diagnosis purposes (small activities) but rather to present new possibility of post-therapeutic imaging (substantially higher activities).

For post-therapeutic imaging after intravenous radiopharmaceutical administration the best spatial resolution offers standard scintigraphic camera for  $^{90}\text{Y}/^{177}\text{Lu}$  DOTATATE imaging, with using  $^{177}\text{Lu}$  photopeaks.

The worst spatial resolution offers standard scintigraphic camera for  $^{90}\text{Y}/^{177}\text{Lu}$  DOTATATE imaging, with using  $^{90}\text{Y}$  *bremsstrahlung* gammas.

**KEY words:** somatostatin receptor,  $^{90}\text{Y}/^{177}\text{Lu}$ -DOTATATE, tandem therapy, PET/CT, imaging

Nuclear Med Rev 2013; 16, 2: 70–74

## Background

Neuroendocrine tumors (NETs) are a heterogeneous group of neoplasms derived from endocrine stem cells. The choice of an appropriate treatment option as far as patients with inoperable or metastatic neuroendocrine tumors are concerned, is limited. These tumors are characterized by overexpression of somatostatin receptors (SSTR), which is utilized for imaging using SSTR analogs [1]. Knowledge of overexpression of somatostatin analogs leads to possibility to use it in diagnosis and radiolabeled therapy. Peptide receptor radionuclide therapy (PRRT) somatostatin analogs labeled with  $^{90}\text{Y}$  and  $^{177}\text{Lu}$  in neuroendocrine tumors (NETs) results in

Correspondence to: Jolanta Kunikowska  
Nuclear Medicine Department, Medical University of Warsaw  
ul. Banacha 1a, 02–097 Warsaw, Poland  
Tel.: +48 22 599 22 70  
Fax: +48 22 599 11 70  
E-mail: [jolanta.kunikowska@wum.edu.pl](mailto:jolanta.kunikowska@wum.edu.pl)

symptomatic improvement, prolonged survival, and enhanced quality of life [2–5]. The post-therapeutic imaging leads to possibility to assess the biodistribution of radiopharmaceuticals. The information is useful for control of treatment, evaluation of dosimetric data or prediction of treatment effects. Such possibility is given by 177Lu fraction of gamma emission. Moreover, 90Y is almost pure beta-emitter (99,999%  $\beta^-$ ) [6], so possibility of post-therapeutic imaging is already widely used in order to qualitatively assess biodistribution using *bremsstrahlung*.

Several studies have reported on the use of high-resolution 90Y PET/CT scans in the evaluation of the biodistribution of 90Y-labeled glass or resin based microspheres after radioembolisation of malignant liver lesions [7–11], but there are no data concerning this method in evaluation of radiopharmaceuticals in other treatment procedures.

The aim of our study was to describe different possibility in post-therapeutic imaging in patients underwent tandem therapy 90Y/177Lu-DOTATATE with preliminary results of 90Y PET imaging.

## Material and methods

The study was approved by the ethical committee of Medical University of Warsaw. All patients gave written informed consent.

### Patients

Thirty patients with histological confirmation of metastatic neuroendocrine tumors (G1 and G2) were treated with tandem therapy 90Y/177Lu-DOTATATE.

The treated group consisted of 11 men and 19 women; the mean age was ( $\pm$  SD):  $55 \pm 10.9$  y (range 39–73). Progressive disease, confirmed by CT and increased blood concentrations of chromogranin A (CgA) were present in both groups.

The response to the treatment was observed in CT and defined according to the Response Evaluation Criteria in Solid Tumors (RECIST criteria).

The following inclusion criteria to the therapy were used:

- somatostatin receptor imaging (99mTc-HYNIC-TATE or 68Ga-DOTATATE) positive uptake in the tumor and metastases at least 3 months before inclusion (qualitative analysis);
- histological confirmation of NET tumor, assessed as inoperable or as metastatic;
- hemoglobin level (Hb)  $\geq 10$  g/dL; Leucocytes (WBC)  $\geq 2 \times 10^9$ /L; thrombocytes (PLT)  $\geq 90 \times 10^9$ /L;
- calculated glomerular filtration rate (GFR)  $> 40$  mL/min;
- Karnofsky Performance Status  $\geq 60$ ;
- life expectancy  $> 3$  months;
- no pregnancy or lactation.

In patients receiving long-acting somatostatin analogs, therapy with somatostatin radiolabeled analogs was performed 5 weeks after completion of therapy with octreotide (Sandostatin LAR; Novartis) and after 3–5 weeks with lanreotide (Somatuline; Somatuline autogel, Ipsen). The interval between chemotherapy and PRRT was at least 3 months.

### Treatment

Therapy was performed on an out-patients basis.

Treatment sessions were repeated, up to a total calculated dose of 7.4 GBq/m<sup>2</sup>. The injected activity per one course equaled 2.2–3.7 GBq.

Regarding 90Y/177Lu-DOTATATE, 50% of the activity was attributed to 90Y-DOTATATE and 50% to 177Lu-DOTATATE. Median period between the treatment courses was 49 days, respectively. A mixed amino-acid (1000 mL Vamin 18, Fresenius Kabi or Aminomel 12,E, Baxter) and Ringer's solutions (500 mL) were infused over 8 hours for kidney protection; with infusion of 200 mL prior to administration of the treatment [12]. Before administration of radiopharmaceutical, ondansetron (8 mg, Zofran, Glaxo Wellcome, Atossa, Anpharm S. A.) had been injected intravenously to prevent nausea and vomiting.

### Post-therapy imaging

According to the physical properties of 90Y and 177Lu for imaging following points are important:

- 90Y is a beta-minus emitter with two decay modes: main with an end-point energy of 2.28 MeV and mean energy 0.93 MeV leading to the 90Zr ground state (99.99%) and rare one with end-point mean of 0.52 MeV and average energy 0.20 MeV (0.011%) leading to the 90Zr excited state at 1.78 MeV, followed by pair creation, a half-life of 64h [6, 13, 14].
- 177Lu is a beta-minus emitter with an end-point energy of 0.498 MeV and mean energy 0.93 MeV (78.6%), a half-life of 6.73 d and gammas emitter mainly with 112 keV (6.5%) and 208 keV (11%) photopeaks [13].

90Y could be imaged on a standard scintigraphic camera or PET scanner, as recent studies have shown [7, 11]. Both uses scintillation phenomena for gamma ray detection. Beta-minus high energy particles can't be detect directly but this devices may be used for imaging of distribution of beta-emitters via *bremsstrahlung* phenomena — gammas produced by the deceleration of a charged particle when deflected by another charged particle, typically an electron by an atomic nucleus [15, 16]. For scintigraphic imaging whole body (WHBA) and single photon emission (SPECT) is used.

For tandem 90Y/177Lu-DOTATATE therapy it is complicated to use spectrum gammas in standard scintigraphic camera.

The components of spectrum are:

- gammas 112 keV and 208 keV photopeaks from 177Lu;
- compton scattering gammas from 177Lu photopeaks;
- *bremsstrahlung* gammas from 177Lu, almost flat over 80–250 keV energy range;
- *bremsstrahlung* gammas from 90Y, almost flat over 80–250 keV energy range.

Imaging possibilities of 90Y in PET scanner comes into existence in a very complex way — there are two subtle phenomena in the decay effecting with beta plus radiation. Firstly, very rarely (0.011%) 90Y decays to 90Zr first excited state that de-excite with pair production, from which positron annihilate producing pair of 511 keV gammas. Secondly, *bremsstrahlung* gammas, emitted from 90Y beta-minus decay, with energy greater than 1.022 MeV can produce positron-electron pairs. Again, positron can annihilate with low-energy thermal electron, with result in two 511 keV gammas. They may be used by PET scanner [15, 16].

## RESULTS

### Patients' characteristics

The study included 30 patients with metastatic neuroendocrine tumors.

This group consists of 15 patients with neuroendocrine foregut tumors, 9 with midgut neuroendocrine tumors, 1 patient with hindgut neuroendocrine tumors and 2 patients with other tumors (1 patient with Multiple Endocrine Neoplasia — MEN 1, 1 patient with Hippel-Landau syndrome), and other 3 with unknown primary tumors.

### Results of therapy

All patients presented progressive disease before 90Y/177Lu-DOTATATE therapy.

Out of all the patients, median OS was 49.8 months and median EFS time 24.3 months.

90Y/177Lu-DOTATATE has been well tolerated, with little acute toxicity — main concern is renal and hematologic function (renal grade 3 and 4 not observed, hematological grade 3 in 2% of patients).

### Results of post-therapy imaging

According the literature and earlier study in our Department we implement following imaging protocols [5].

For imaging 177Lu component of 90Y/177Lu-DOTATATE tandem with scintigraphic camera the 177Lu photopeaks are used. WHBA scan and SPECT acquisition of the abdomen were performed 24 hours post therapy injection, using the dual-head Varicam camera (ELSCINT). Acquisition was made with energy window  $\pm 10\%$  centered on 208 keV, with a parallel-hole, high-energy, general-purpose collimators. In case of WHBA continuous acquisition parameters are:  $256 \times 256$  matrix, 8 cm/min. In case of SPECT acquisition parameters are:  $128 \times 128$  matrix, zoom 1.28,  $60 \times 6^\circ \times 60$  sec, iterative OSEM 2D reconstruction with Chang attenuation correction method and Gauss 6mm filter.

In case post-therapeutic imaging with 90Y/177Lu DOTATATE tandem, acquisition protocol is fully exploiting abilities of the contemporary scintigraphic camera.

Spatial resolution achieved in these conditions, measured using the phantom of the torso filled up with water, is not worse than 8 mm FWHM. In our study spatial resolution in human body was about 15 mm.

For imaging 90Y component of 90Y/177Lu-DOTATATE tandem with scintigraphic camera the *bremsstrahlung* phenomena was used. Imaging was performed 24 hours post-therapy using the dual-head Varicam camera (ELSCINT). Energy window was centered on 100 keV  $\pm 35\%$  window width, and with a parallel-hole, low-energy, high resolution collimators. WHBA scans in  $256 \times 256$  matrix, 8 cm/min was performed.

Spatial resolution achieved in these conditions, measured with using the phantom of the torso filled up with water, is not worse than 20 mm FWHM. In our study spatial resolution in human body was highly depending on localization of metastasis in liver — for peripheral regions 25 mm and for hilum of liver 35–40 mm.

For imaging 90Y component of 90Y/177Lu-DOTATATE tandem with PET scanner an attempt of acquisition was made. Data were acquired on Siemens Biograph Truepoint PET/CT (window 511 keV  $\pm 15\%$ ) 4 hours after 90Y/177Lu-DOTATATE administration. 30 min PET scanning (one bed position centered on the liver) with low dose CT was performed for attenuation correction. The PET data were reconstructed using a TRUEx algorithm (2 iterations, 14 subsets) with  $168 \times 168$  matrix.

Number of electron-positron pairs, which occurs, is very small compared to the number of  $\beta$ -particles emitted by 90Y (about  $32 \times 10^{-6}$  511 keV gammas pairs for one  $\beta$ -particle in theory [6, 13]. In this experiment, despite the high activity (approximately 4 GBq) the number of recorded true coincidence events constituting the image is low, and amount about 100 per sec true coincidences in comparison about 106 per sec gammas collected by the detector. An important advantage is a possibility of obtaining a resolution of modern PET scanner. For Biograph 64 SIEMENS PET scanner it is about 5 mm FWHM. The resolution in our study was about 25–30 mm. Figure 1 is shown post-therapeutic different imaging techniques of the evaluation of biodistribution 90Y/177Lu-DOTATATE.

### Discussion

In radioisotope therapy pure beta-emitting radionuclides are used to deliver an intense, local radiation dose to the target tissue. In the past 90Y imaging was limited to distribution of 90Y-labeled radiopharmaceuticals in spaces such as the abdominal cavity and joints after local injections [17]. The spatial and energy dependence of *bremsstrahlung* production causes an inherent limitation in spatial resolution for *bremsstrahlung* imaging. While high-energy photons are created near the decay site, most low-energy *bremsstrahlung* photons are produced further from the 90Y decay location.

For imaging 90Y component of 90Y/177Lu-DOTATATE tandem with scintigraphic camera the *bremsstrahlung* phenomena was used. Should to emphasize, that in this phenomena gammas come into existence in tissues surrounding activity source. In the end meaning worsening the spatial resolution is taking place, in our cases the received spatial resolution was 30 mm. The *bremsstrahlung* phenomena was in the literature successfully used for loco-regional deposition of 90Y-radiopharmaceuticals [19, 20], but after intravenous application of 90Y-peptides due to low spatial resolution it is not used for dosimetry study. It should be noted that the diagnostic point of view image shows the *bremsstrahlung* gammas coming into existence in tissues surrounding the source of the radiation, which degrades the resolution slightly.

177Lu imaging component of 90Y/177Lu-DOTATATE tandem therapy with scintigraphic camera the 177Lu photopeaks were used. Energy window 208 keV  $\pm 10\%$  giving the following benefits:

- in view of a large number of registered gammas significant shortening the time of performing the examination is possible. In the end also a plausibility of coming into existence of patient moving artifacts is decreasing;
- it is minimizing coming into existence of artifacts dating from Compton scattering;
- a participation is curbing *bremsstrahlung* phenomena in the presence beta-emitters 90Y and 177Lu, which is a reason for degradation the spatial resolution.

With the use of low-energy  $\beta$ -components emitted by 177Lu, not only post-treatment scans can be acquired, but individual dosimetric data can also be obtained. The absorbed radiation doses to dose-limiting organs such as the kidneys and bone marrow are calculated to better tailor the total cumulative activity that can be administered to the individual patient [18].

For imaging 90Y component of 90Y/177Lu-DOTATATE tandem with PET scanner an attempt of acquisition was made.

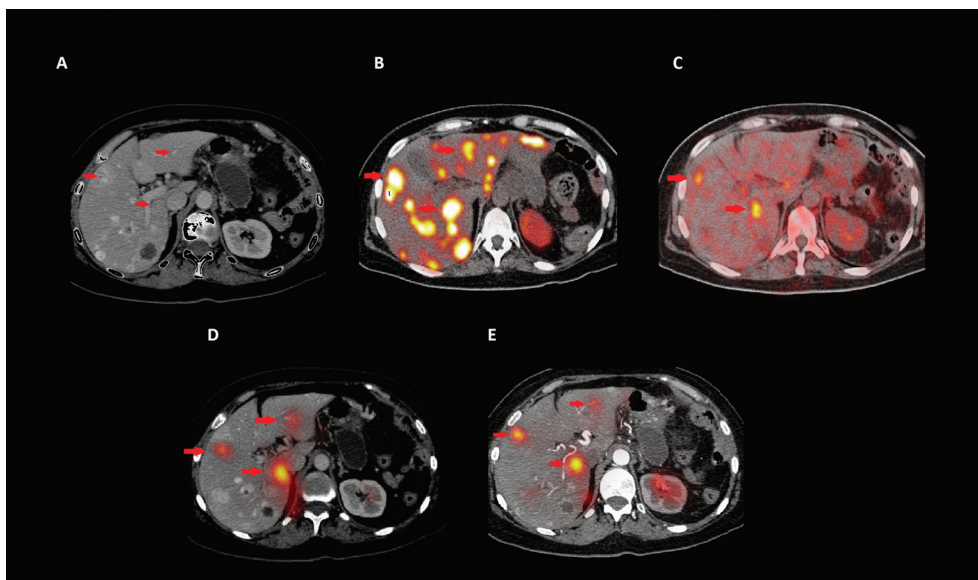


**Figure 1.** A 64-years-old woman after surgery of primary tumors localized in pancreas: **A.** Pre-therapeutic liver metastases in the angio-CT of abdomen; **B.** Qualification to therapy PET/CT with  $^{68}\text{Ga}$  DOTATATE with disseminated metastases in the liver and peritoneal cavity; **C.** Post-therapeutic PET scanning 4 hours after  $^{90}\text{Y}/^{177}\text{Lu}$ -DOTATATE administration; **D.** Post-therapeutic SPECT with  $^{90}\text{Y}$  bremsstrahlung phenomena, 24 hours after injection; **E.** Post-therapeutic SPECT of the abdomen with energy window centered on  $^{177}\text{Lu}$  photopeak 24 hours after injection

Despite such low quantum efficiency reliably diagnostic images was achieved. An important advantage is to obtain a four times better resolution with respect a resolution use in SPECT cameras which is about 20 mm (see C and D in Figure 1). Theoretically it seems that in centers with a PET scanner the use of  $^{90}\text{Y}$  as a primary post-therapeutic imaging method should be considered. In our approach should be emphasized that the  $^{90}\text{Y}$ -labeled therapeutic agent was given intravenously by the vein. Therefore PET/CT imaging can reveal not only the distribution of local activity, but also general systemic biodistribution of tracer, however because of low number of electron-positron pairs it is not possible to receive whole body image for acceptable time. Our study focused on liver imaging to determine whether this method of imaging provides measurable benefits. In PET/CT imaging using the  $^{90}\text{Y}$ -labeled therapeutic agent should pay attention to the fact that the ratio of signal to noise ratio is small, because the image consists of a small number of true coincidence events. In the case of locally administered high activity of  $^{90}\text{Y}$ -labeled glass it could be expect high-resolution image, and thus a better quality of imaging [7–11]. Unfortunately in case of systemic administered activity, this resolution is 25–30 mm, because of lower energy deposited in the liver. On the literature data  $^{90}\text{Y}$ -DOTATOC systemic administration did not permit to obtain suitable PET imaging, whereas  $^{90}\text{Y}$ -DOTATOC directly injected into the surgical cavity by locoregional route in glioma treatment provide excellent imaging both PET and SPECT techniques [21].

## Conclusions

The theoretically best spatial resolution (about 5–6 mm FWHM in phantom but 25–30 mm in human body) offers PET scanner, however it is important to keep in mind that  $^{90}\text{Y}$ -imaging PET is not used for diagnosis purposes (small activities) but rather to

present new possibility of post-therapeutic imaging (substantially higher activities).

The medium spatial resolution (about 8–10 mm FWHM in phantom and 15 mm in human body) offers standard scintigraphic camera for  $^{90}\text{Y}/^{177}\text{Lu}$  DOTATATE imaging, with using  $^{177}\text{Lu}$  photopeaks.

The worst spatial resolution (about 20 mm FWHM in phantom and 30 mm in human body) offers standard scintigraphic camera for  $^{90}\text{Y}/^{177}\text{Lu}$  DOTATATE imaging, with using  $^{90}\text{Y}$  bremsstrahlung gammas.

## References

1. Reubi JC. Peptide receptors as molecular targets for cancer diagnosis and therapy. *Endocr Rev* 2003; 24: 389–427.
2. Kwekkeboom DJ, de Herder WW, Kam BL et al. Treatment with the radiolabeled somatostatin analog [ $^{177}\text{Lu}$ -DOTA $_0$ , Tyr $_3$ ]octreotate: toxicity, efficacy, and survival. *J Clin Oncol* 2008; 26: 2124–2130.
3. Imhof A, Brunner P, Marincek N et al. Response, survival, and long-term toxicity after therapy with the radiolabeled somatostatin analogue [ $^{90}\text{Y}$ -DOTA]-TOC in metastasized neuroendocrine cancers. *J Clin Oncol* 2011; 29: 2416–2423.
4. Imhof A, Brunner P, Marincek N et al. Response, survival, and long-term toxicity after therapy with the radiolabeled somatostatin analogue [ $^{90}\text{Y}$ -DOTA]-TOC in metastasized neuroendocrine cancers. *J Clin Oncol* 2011; 29: 2416–2423.
5. Kunikowska J, Króllicki L, Hubalewska-Dydejczyk A et al. Clinical results of radionuclide therapy of neuroendocrine tumours with  $^{90}\text{Y}$ -DOTATATE and tandem  $^{90}\text{Y}/^{177}\text{Lu}$ -DOTATATE: which is a better therapy option? *Eur J Nucl Med Mol Imaging* 2011; 38: 1788–1797.
6. Selwyn RG, Nickles R, Thomadsen BR, DeWerd LA, Micka JA. A new internal pair production branching ratio of  $^{90}\text{Y}$ : the development of a non-destructive assay for  $^{90}\text{Y}$  and  $^{90}\text{Sr}$ . *Appl Radial Isot* 2007; 65: 318–327.
7. Lhommel R, Goffette P, Van den Eynde M et al. Yttrium-90 TOF PET scan demonstrates high-resolution biodistribution after liver SIRT. *Eur J Nucl Med Mol Imaging* 2009; 36: 1696.

8. Lhommel R, van Elmbt L, Goffette P et al. Feasibility of yttrium-90 TOF-PET based dosimetry in liver metastasis therapy using SIR-spheres. *Eur J Nucl Med Mol Imaging* 2010; 37: 1654–1662.
9. Werner MK, Brechtel K, Beyer T, Dittmann K, Pfannenbergl C, Kupferschläger J. PET/CT for the assessment and quantification of <sup>90</sup>Y biodistribution after selective internal radiotherapy (SIRT) of liver metastases. *Eur J Nucl Med Mol Imaging* 2010; 37: 407–408.
10. Lhommel R, Walrand S, van Elmbt L, Pauwels S, Jamar F. Dose-response relationship in liver-SIRT: <sup>90</sup>Y TOF-PET versus <sup>99m</sup>Tc-MAA SPECT based dosimetry. *Eur J Nucl Med Mol Imaging* 2010; 37: S201.
11. Gates VL, Esmail AAH, Marshall K, Spies S, Salem R. Internal pair production of <sup>90</sup>Y permits hepatic localization of microspheres using routine pet: proof of concept. *J Nucl Med* 2010; 52: 72–76.
12. Jamar F, Barone R, Mathieu I et al. <sup>86</sup>Y-DOTA0-D-Phe1-Tyr3-octreotide (SMT487): a phase 1 clinical study — pharmacokinetics, biodistribution and renal protective effect of different regimens of amino acid co-infusion. *Eur J Nucl Med Mol Imaging* 2003; 30: 510–518.
13. Nickles RJ, Roberts AD, Nye JA, Converse AK, Barnhart TE, et al. Assaying and PET imaging of yttrium-90: 1.34 ppm.0. *Conf Record of IEEE Nuclear Science Symp and Medical Imaging Conf* 2004; 3412–3414.
14. Table of Nuclei, Nuclear Data Center, Korea Atomic Energy Research Institute 2000, <http://atom.kaeri.re.kr> (last access 30.05.2013).
15. Kao YH, Steinberg J, Yan J et al. Optimization of Yttrium-90 Processing on a Clinical PET/CT System 2011 IEEE Nuclear Science Symposium Conference Record. doi: 10.1109/NSSMIC.2011.6154488.
16. Shen S, DeNardo GL, Yuan A, DeNardo DA, DeNardo SJ. Planar gamma camera imaging and quantitation of yttrium-90 bremsstrahlung. *J Nucl Med* 1994; 35: 1381–1389.
17. Baechler S, Camus F, Haag G et al. SPECT and PET Imaging of Yttrium-90 in Targeted Radionuclide Therapy Swiss Society of Radiobiology and Medical Physics, Annual General Meeting 2011.
18. Wehrmann C, Senfleben S, Zachert C, Muller D, Baum RP. Results of individual patient dosimetry in peptide receptor radionuclide therapy with <sup>177</sup>Lu-DOTA-TATE and <sup>177</sup>Lu-DOTA-NOC. *Cancer Biother Radiopharm* 2007; 22: 406–416.
19. Fabbri C, Sarti G, Cremonesi M et al. Quantitative analysis of <sup>90</sup>Y bremsstrahlung SPECT-CT images for application to 3D patient-specific dosimetry. *Cancer Biother Radiopharm* 2009; 24: 145–153.
20. Fabbri C, Mattone V, Sarti G et al. <sup>90</sup>Y-based PET and SPECT/CT imaging in locoregional brain treatment for high-grade gliomas: retrospective fusion with MRI. *Eur J Nucl Med Mol Imaging* 2012; 39: 1822–1823.
21. Fabbri C, Mattone V, Casi M et al. Quantitative evaluation on <sup>90</sup>Y DOTATOC PET and SPECT imaging by phantom acquisitions and clinical applications in locoregional and systemic treatments. *Q J Nucl Med Mol Imaging*. 2012; 56: 522–528.